

# GAIT RECOGNITION VIA COLLABORATING DISCRIMINATIVE AND GENERATIVE DIFFUSION MODELS

Haijun Xiong Bin Feng <sup>†</sup> Bang Wang Xinggang Wang Wenyu Liu

School of EIC, Huazhong University of Science & Technology  
 {xionghj, fengbin}@hust.edu.cn

## ABSTRACT

Gait recognition offers a non-intrusive biometric solution by identifying individuals through their walking patterns. Although discriminative models have achieved notable success in this domain, the full potential of generative models remains largely underexplored. In this paper, we introduce **CoD<sup>2</sup>**, a novel framework that combines the data distribution modeling capabilities of diffusion models with the semantic representation learning strengths of discriminative models to extract robust gait features. We propose a Multi-level Conditional Control strategy that incorporates both high-level identity-aware semantic conditions and low-level visual details. Specifically, the high-level condition, extracted by the discriminative extractor, guides the generation of identity-consistent gait sequences, whereas low-level visual details, such as appearance and motion, are preserved to enhance consistency. Furthermore, the generated sequences facilitate the discriminative extractor’s learning, enabling it to capture more comprehensive high-level semantic features. Extensive experiments on four datasets (SUSTech1K, CCPG, GREW, and Gait3D) demonstrate that CoD<sup>2</sup> achieves state-of-the-art performance and can be seamlessly integrated with existing discriminative methods, yielding consistent improvements.

## 1 INTRODUCTION

Gait recognition is a biometric technology that distinguishes individuals based on unique walking patterns. Unlike other biometric modalities, such as face, iris, and fingerprint recognition, gait can be captured from a distance without requiring subject cooperation, making it particularly suitable for applications in crime prevention, sports science, and healthcare (Venkat & De Wilde, 2011; Sepas-Moghaddam & Etemad, 2022). Despite significant progress in gait recognition, existing discriminative methods (Wang et al., 2023c; Ye et al., 2024; Xiong et al., 2025) (Figure 1 (a)) continue to struggle in complex scenarios involving variations in clothing, viewpoints, occlusions, and carried objects, which complicate the extraction of robust discriminative features.

Generative models, particularly diffusion models (Ho et al., 2020; Song et al., 2021), have recently gained significant attention for their remarkable capability to generate high-quality images, visually compelling images. These models excel at capturing complex data distributions and generate realistic samples by iteratively reversing a noise injection process. Beyond image synthesis, the potential of diffusion models has been increasingly explored in video generation (Ho et al., 2022), where they effectively capture temporal coherence and high-level structural dynamics. Such characteristics make them especially suitable for tasks that demand both realistic visual generation and consistent motion evolution, including video synthesis and dynamic scene modeling (Yu et al., 2024; Wu et al., 2025). Furthermore, due to their powerful representational capacity, recent works have leveraged pre-trained diffusion models for a variety of downstream applications, achieving promising results in pose estimation (Feng et al., 2023), mesh recovery (Zhu et al., 2024; Foo et al., 2023), and action recognition (Wu et al., 2024a; Li et al., 2023a).

---

<sup>†</sup>Corresponding author.

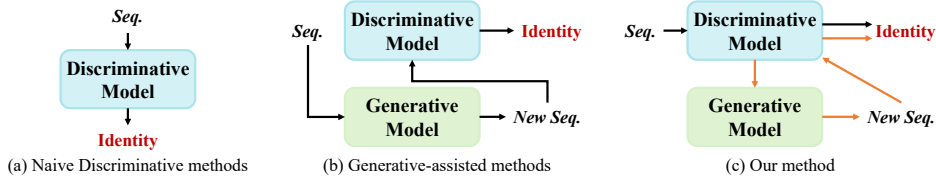


Figure 1: **Comparison of different methods for gait recognition.** (a) Naive discriminative methods, such as GaitSet (Chao et al., 2019); (b) Generative-assisted methods, such as DenoisingGait (Jin et al., 2025); (c) Our proposed CoD<sup>2</sup>, which integrates collaborating discriminative and generative models.

Previous studies (Jin et al., 2025) (Figure 1 (b)) have employed diffusion models to denoise RGB gait sequences and generate clean gait representations. However, such methods do not fully exploit the intrinsic relationship between generative and discriminative models, thereby limiting the potential of the generative model. While discriminative models emphasize inter-class separability, generative models focus on modeling the underlying data distribution. These two paradigms provide complementary perspectives on the data, and their integration can yield a more holistic understanding of gait patterns. Consequently, combining discriminative models with generative diffusion models is essential for enhancing the feature extraction capabilities of both, ultimately leading to more effective gait recognition.

To address these aforementioned challenges, we propose a novel gait recognition framework, **CoD<sup>2</sup>**. As illustrated in Figure 1 (c), CoD<sup>2</sup> differs fundamentally from prior works by integrating the data distribution modeling capability of diffusion models with the semantic representation learning strength of discriminative models, thereby extracting more robust gait features. We further present a Multi-level Conditional Control strategy that combines both high-level and low-level conditions to guide the generative learning process of the diffusion model. Specifically, the high-level condition, derived from the discriminative feature extractor, provides identity-aware semantic information to generate identity-consistent gait sequences. In contrast, the low-level condition preserves essential visual details, such as appearance and motion information, which are critical for maintaining identity consistency in the generated sequences. Moreover, the generated sequences in turn promote the training of the discriminative extractor, enabling it to capture richer and more comprehensive semantic representations. We evaluate CoD<sup>2</sup> through extensive experiments on four datasets (Shen et al., 2023; Li et al., 2023b; Zhu et al., 2021; Zheng et al., 2022b), achieving state-of-the-art Rank-1 performance. Furthermore, integrating CoD<sup>2</sup> with four representative discriminative methods (Chao et al., 2019; Lin et al., 2021; Fan et al., 2023; 2025) consistently improves performance across all datasets, demonstrating its strong versatility. Notably, CoD<sup>2</sup> introduces only a marginal increase in training consumption, with no impact on testing efficiency. In summary, the main contributions are as follows:

- We introduce CoD<sup>2</sup>, a novel gait recognition framework that integrates the data distribution modeling capacity of generative diffusion models with the semantic representation learning ability of discriminative models, enhancing gait feature extraction through their complementary strengths.
- We propose a Multi-level Conditional Control strategy that jointly leverages high-level identity-aware semantic features with low-level visual details to guide the diffusion model’s generative process. The generated sequences facilitate the discriminative model’s learning, further improving feature robustness.
- Extensive experiments demonstrate that CoD<sup>2</sup> achieves state-of-the-art performance and can be seamlessly integrated with existing discriminative methods, consistently improving performance with minimal impact on training consumption and no effect on testing efficiency.

## 2 RELATED WORK

### 2.1 GAIT RECOGNITION

Current gait recognition methods can be broadly categorized into model-based and appearance-based methods, depending on the input modality.

Model-based methods (Teepe et al., 2021; 2022; Li & Zhao, 2022; Fu et al., 2023) exploit structural human priors, such as skeletons and 3D meshes. For example, PoseGait (Liao et al., 2020) integrates multiple skeleton-based features with human prior knowledge to enhance recognition performance, while CAG (Huang et al., 2023) employs adaptive conditional networks to extract fine-grained representations. Other studies (Pinyoanuntapong et al., 2023; Zhang et al., 2023a) adopt transformer architectures to capture long-range spatial dependencies, and SMPLGait (Zheng et al., 2022b) further improves recognition by utilizing dense 3D mesh representations reconstructed from RGB images.

Appearance-based methods (Fan et al., 2023; Wang et al., 2024; Ma et al., 2023; Peng et al., 2024a; Zheng et al., 2022a; Wang et al., 2023b; Zheng et al., 2023; Xiong et al., 2024a; Zheng et al., 2024) directly learn spatial-temporal representations from gait silhouettes or RGB sequences. Gait-Set (Chao et al., 2019) is the first to treat gait sequences as unordered frame sets. Subsequent methods (Fan et al., 2020; Huang et al., 2021; Lin et al., 2021) adopt 1D or 3D CNNs to model local motion patterns across frames, while deeper architectures (Ma et al., 2024; Fan et al., 2025) have been developed to extract richer identity-discriminative features. Recent studies (Dou et al., 2023; Wang et al., 2023a; Xiong et al., 2024b) revisit gait recognition from a causal inference perspective, and DenoisingGait (Jin et al., 2025) employs diffusion models to generate noise-free gait representations. Moreover, alternative modalities, such as point clouds and RGB videos, have recently been incorporated into gait recognition frameworks (Shen et al., 2023; Ye et al., 2024), broadening the scope of this research field.

## 2.2 DIFFUSION MODELS FOR REPRESENTATION LEARNING

Diffusion models have emerged as a powerful paradigm for generative modeling, particularly in image and video synthesis (Ho et al., 2020; 2022). These models generate high-quality visual content by progressively refining Gaussian noise through an iterative denoising process. Building on their remarkable success, recent studies have extended diffusion models to a wide range of downstream tasks (Xu et al., 2024; Wu et al., 2024a; Feng et al., 2023; Chen et al., 2023; Vogel et al., 2024; Toker et al., 2024; Kara et al., 2024; Wu et al., 2024b). For example, DPMesh (Zhu et al., 2024) leverages spatial structural priors from pre-trained diffusion models to reconstruct occluded human meshes, while HOIAnimator (Song et al., 2024) introduces Perceptive Diffusion Models to enhance the realism of human-object interactions in animations. Moreover, ControlNet (Zhang et al., 2023b) integrates spatial conditioning mechanisms into pre-trained diffusion models for precise detail manipulation, and AYG (Ling et al., 2024) combines Gaussian Splatting with diffusion models to enable text-to-4D generation.

In this paper, we propose CoD<sup>2</sup>, the first framework that enhances feature extraction by unifying the semantic representation learning capability of discriminative models and the data distribution modeling power of generative models.

## 3 METHODOLOGY

### 3.1 BACKGROUND

Before introducing our proposed method, we briefly review the key concepts of gait recognition and the Denoising Diffusion Probabilistic Model (DDPM) (Ho et al., 2020).

**Discriminative Gait Recognition.** Given a gait sequence  $\mathbf{X}_0 \in \mathbb{R}^{1 \times T \times H \times W}$  with  $T$  frames, each of size  $(H, W)$ , discriminative gait recognition methods typically process  $\mathbf{X}_0$  through a discriminative feature extractor  $\mathcal{D}$  to obtain the identity representation  $\mathbf{f}_I \in \mathbb{R}^{C \times p}$ , where  $C$  and  $p$  denote the number of channels and parts, respectively:

$$\mathbf{f}_I = \mathcal{D}(\mathbf{X}_0). \quad (1)$$

Subsequently,  $\mathbf{f}_I$  is refined using a separate fully connected (S-FC) layer followed by BNNeck, and optimized with a combination of triplet and cross-entropy losses:

$$\mathcal{L}_D = \mathcal{L}_{tri} + \mathcal{L}_{ce}. \quad (2)$$

**DDPM.** DDPM generates high-quality visual content by iteratively denoising random Gaussian noise. It consists of two phases: a fixed forward diffusion process and a learnable reverse denoising

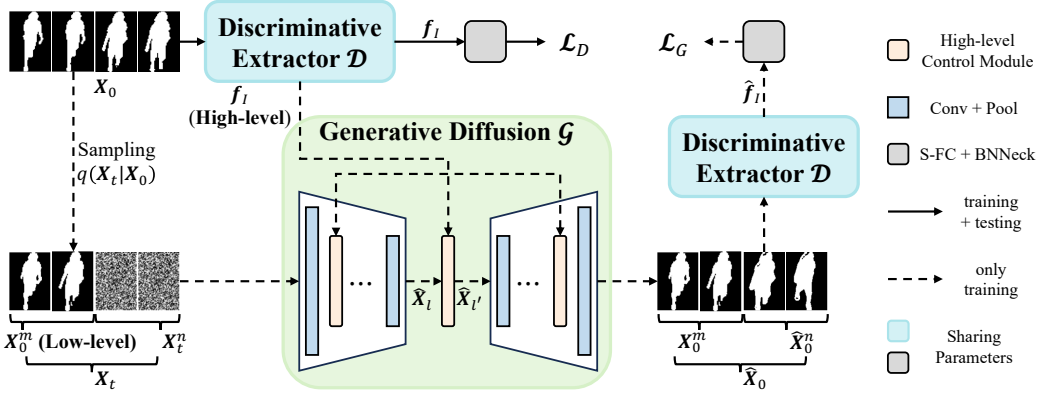


Figure 2: **Overview of our proposed method.** The discriminative extractor  $\mathcal{D}$  (e.g., GaitSet, GaitGL, GaitBase, or DeepGaitV2) first extracts the identity feature  $f_I$  from the input gait sequence  $\mathbf{X}_0$ . This feature serves as a high-level semantic condition to guide the generative diffusion model  $\mathcal{G}$  during sequence generation. The noise sequence  $\mathbf{X}_t$  is composed of Gaussian noise  $\mathbf{X}_t^n \sim \mathcal{N}(0, I)$  and low-level visual information  $\mathbf{X}_0^m$  sampled from  $\mathbf{X}_0$ . The generated gait sequence  $\hat{\mathbf{X}}_0$  is then processed by  $\mathcal{D}$  to extract its identity feature  $\hat{f}_I$ . Finally,  $\mathcal{D}$  and  $\mathcal{G}$  are jointly optimized with the loss  $\mathcal{L}_D$  and  $\mathcal{L}_G$ , where  $\mathcal{G}$  is employed only for training, while  $\mathcal{D}$  is used for both training and inference.

process. In the forward phase, Gaussian noise is gradually added to the original image  $x_0$  through a Markov chain, progressively transforming it into pure Gaussian noise  $x_T \sim \mathcal{N}(0, I)$ . At each timestep  $t$ , the noised variable  $x_t$  depends only on its previous state  $x_{t-1}$ , as formulated by:

$$q(x_t|x_{t-1}) = \mathcal{N}(x_t; \sqrt{1 - \beta_t}x_{t-1}, \beta_t I), \quad (3)$$

where  $\beta_t$  denotes a predefined variance schedule. The reverse process reconstructs  $x_0$  from  $x_T$  through iterative denoising:

$$p_\theta(x_{t-1}|x_t) = \mathcal{N}(x_{t-1}; \mu_\theta(x_t, t), \sigma_t^2 I), \quad (4)$$

where  $\mu_\theta(x_t, t)$  is a parameterized function, typically implemented as a neural network, used to predict the mean  $\hat{\mu}$  at each timestep. Recent methods, such as ControlNet (Zhang et al., 2023b), extend diffusion models to controllable generation by incorporating conditional input. Given a condition  $c$ , the training objective can be formulated as:

$$\min_{\theta} \mathbb{E}_{x_0, c, t, \mu} \left[ \|\mu - \mu_\theta(x_t, c, t)\|_2^2 \right], \quad (5)$$

which enables the generation of realistic samples from Gaussian noise.

### 3.2 PIPELINE

The overall framework of CoD<sup>2</sup> is illustrated in Figure 2. It comprises two discriminative extractors with shared parameters, and a generative diffusion module. Similar to previous methods, the first discriminative extractor  $\mathcal{D}$  processes the input gait sequence  $\mathbf{X}_0$  to obtain the identity feature  $f_I$ . Meanwhile, a noise sequence  $\mathbf{X}_t$  is constructed by combining the low-level condition  $\mathbf{X}_0^m$  (a part of  $\mathbf{X}_0$ ) with Gaussian noise  $\mathbf{X}_t^n$ . The identity feature, serving as a high-level condition, guides the denoising process of the generative diffusion module  $\mathcal{G}$  by embedding identity-aware semantic information, resulting in a generated gait sequence  $\hat{\mathbf{X}}_0$ . The second extractor  $\mathcal{D}$  is then reapplied to extract the identity feature  $\hat{f}_I$  from  $\hat{\mathbf{X}}_0$ , ensuring identity consistency. This bidirectional interaction between  $\mathcal{D}$  and  $\mathcal{G}$  not only reinforces the generative module but also enhances the discriminative extractor’s ability to capture more effective gait features.

### 3.3 DISCRIMINATIVE EXTRACTOR AND GENERATIVE DIFFUSION MODULE

The discriminative extractor  $\mathcal{D}$  serves as the core backbone and can be instantiated with various existing gait recognition models, such as GaitSet, GaitGL, GaitBase, and DeepGaitV2-P3D (abbreviated as DeepGaitV2). The versatility of our method is further validated in Table 5. Considering

that binary silhouette sequences are substantially simpler than RGB inputs and that directly predicting noise from noisy sequences provides limited discriminative information (Wu et al., 2024a; Guo et al., 2024), we adopt a lightweight generative diffusion module  $\mathcal{G}$  to generate new sequences from noise. The architectural details of  $\mathcal{G}$  are presented in [Appendix A](#).

### 3.4 MULTI-LEVEL CONDITIONAL CONTROL

The generative diffusion module  $\mathcal{G}$  takes the noise sequence  $\mathbf{X}_t$  and the identity feature  $\mathbf{f}_I$  as input. Here,  $\mathbf{f}_I$  serves as a high-level control condition, encapsulating identity-aware semantic information. Meanwhile,  $\mathbf{X}_0^m$  in  $\mathbf{X}_t$ , derived from the original sequence  $\mathbf{X}_0$ , preserves low-level visual cues (such as appearance and motion), acting as a low-level control condition during the denoising process.

**Low-level conditional control.** Unlike text-to-video generation, gait sequence generation requires preserving visual details from original sequences, such as appearance and motion information. To achieve this, we introduce a sampling strategy that randomly selects continuous  $m$  frames from  $\mathbf{X}_0$  as a reference, denoted as  $\mathbf{X}_0^m \in \mathbb{R}^{1 \times m \times H \times W}$ . This reference is concatenated with Gaussian noise  $\mathbf{X}_t^n \in \mathbb{R}^{1 \times (T-m) \times H \times W}$  along the temporal dimension to construct the noise sequence  $\mathbf{X}_t \in \mathbb{R}^{1 \times T \times H \times W}$ , formulated as:

$$\begin{aligned}\mathbf{X}_0^m &= \mathbf{X}_0[k : k+m], k \in [0, T-m], \\ \mathbf{X}_t^n &= \text{Sample}(\mathcal{N}(0, I)), \\ \mathbf{X}_t &= \text{Cat}(\mathbf{X}_0^m, \mathbf{X}_t^n),\end{aligned}\tag{6}$$

where  $\text{Cat}(\cdot)$  denotes the concatenation operation. During denoising, the spatial-temporal modeling process transfers low-level visual cues from  $\mathbf{X}_0^m$  to  $\mathbf{X}_t^n$ , ensuring that the generated sequences retain essential appearance and motion details. Inspired by LAMP (Wu et al., 2023), we keep the reference frames  $\mathbf{X}_0^m$  noise-free during training, meaning that  $\mathbf{X}_0^m$  remains unchanged after passing through a 3D convolutional layer in  $\mathcal{G}$ , *i.e.*,

$$\left[ \hat{\mathbf{X}}_0^m, \hat{\mathbf{X}}_i^n \right] = \text{Conv}([\mathbf{X}_0^m, \mathbf{X}_i^n]), \quad \hat{\mathbf{X}}_0^m = \mathbf{X}_0^m,$$

which preserves both temporal identity consistency and the integrity of low-level visual details during denoising. By preserving low-level details, this strategy enhances control effectiveness and improves the overall sequence generation.

**High-level conditional control.** The high-level condition embeds identity-aware semantic information into the generative diffusion module  $\mathcal{G}$ , providing effective guidance during the generation process. While ControlNet (Zhang et al., 2023b) performs element-wise addition for condition fusion after convolutional layers, we find this operation too coarse for gait sequence generation, leading to degraded performance (as shown in [Table 7](#)). To address this limitation, we propose a refined High-level Control Module that seamlessly integrates  $\mathbf{f}_I$  into  $\mathcal{G}$ , facilitating identity-aware guidance and improving the generated sequences of generated sequences (as illustrated in [Figure 3](#)).

We draw inspiration from Euler's formula:

$$e^{i\theta} = \cos(\theta) + i \sin(\theta),\tag{7}$$

which represents a signal as a rotation in the complex plane, thereby encoding both amplitude and phase information. Motivated by this, we design a phase modulation module based on sinusoidal projection to effectively embed high-level identity semantics into the generative process.

Specifically, given an intermediate noisy sequence  $\hat{\mathbf{X}}_l \in \mathbb{R}^{C' \times T \times H \times W}$  from the reverse diffusion process, we compute a spatially varying phase feature  $\mathbf{f}_d$  conditioned on the identity feature  $\mathbf{f}_I$ :

$$\mathbf{f}_d = 2\pi \cdot \text{Norm}(\text{Conv}(\hat{\mathbf{X}}_l \cdot \text{S-Fc}(\mathbf{f}_I))).\tag{8}$$

Here,  $S\text{-FC}(\mathbf{f}_I)$  denotes a spatially broadcasted identity embedding, and  $\text{Norm}(\mathbf{x}) = \frac{\mathbf{x} - \mathbf{x}_{\min}}{\mathbf{x}_{\max} - \mathbf{x}_{\min}}$  normalizes the values to the range  $[0, 2\pi]$  via min-max normalization. We then apply sinusoidal modulation to inject identity-aware semantics into the sequence:

$$\hat{\mathbf{X}}_{l'} = \hat{\mathbf{X}}_l \cdot \cos(\mathbf{f}_d) + \boldsymbol{\lambda} \cdot \hat{\mathbf{X}}_l \cdot \sin(\mathbf{f}_d), \quad (9)$$

where  $\boldsymbol{\lambda} \in \mathbb{R}^{C'}$  is a learnable channel-wise scaling vector. This formulation, grounded in Euler's identity (Equation 7), effectively modulates the intermediate representation  $\hat{\mathbf{X}}_l$  with a phase shift parameterized by  $\mathbf{f}_I$ .

This identity-conditioned phase modulation enables the network to impose global semantic control in a spatially adaptive manner. As shown in Figure 3, the sinusoidal components allow smooth and differentiable injection of identity semantics, facilitating the generation of identity-consistent gait sequences.

By jointly incorporating high-level semantic and low-level visual conditions, our method ensures that the generated sequence  $\hat{\mathbf{X}}_0$  preserves appearance and motion details while maintaining strong identity consistency, thereby enhancing discriminative effectiveness.

### 3.5 TRAINING OBJECTIVE

After obtaining the identity features  $\mathbf{f}_I$  and  $\hat{\mathbf{f}}_I$ , we adopt a joint loss  $\mathcal{L}$  to simultaneously optimize the discriminative extractor and the generative diffusion module. The overall objective is formulated as:

$$\mathcal{L} = \mathcal{L}_D + \mathcal{L}_G, \quad (10)$$

where  $\mathcal{L}_D$  (defined in Equation 2) supervises  $\mathbf{f}_I$ , while  $\mathcal{L}_G = \mathcal{L}_{tri} + \mathcal{L}_{ce}$  is applied to supervise the identity feature  $\hat{\mathbf{f}}_I$  of the generated sequence to enforce identity consistency.

## 4 EXPERIMENTS

In this section, we first describe the datasets used and implementation details. We then conduct extensive experiments to evaluate CoD<sup>2</sup>, including both quantitative and qualitative analyses. Finally, comprehensive ablation studies on four datasets are performed to assess the contribution of each component within CoD<sup>2</sup>. More experiments are provided in Appendix B.

### 4.1 DATASETS AND EVALUATION METRICS

**Datasets:** We evaluate our method on four widely used datasets: SUSTech1K (Shen et al., 2023), CCPG (Li et al., 2023b), GREW (Zhu et al., 2021), and Gait3D (Zheng et al., 2022b). SUSTech1K, collected in laboratory, includes conditions such as normal, clothing changes, night, and occlusion. CCPG is designed for cross-domain evaluation, comprising four clothing-change scenarios (*i.e.*, full-body, upper-body, lower-body, and backpacks changes). GREW and Gait3D are large-scale real-world datasets with significant challenges due to diverse environmental conditions. All training and testing splits strictly follow the official dataset protocols.

**Metrics:** Following prior work (Xiong et al., 2024b), we use Rank- $k$  accuracy (R- $k$ ) and mean Average Precision (mAP) to evaluate the performance of CoD<sup>2</sup>.

### 4.2 IMPLEMENTATION DETAILS

(1) All images are resized to  $64 \times 44$ , and an ordered sampling strategy with a fixed sequence length of 30 frames is adopted during training. (2) We primarily employ DeepGaitV2 (Fan et al., 2025) as the discriminative extractor to validate CoD<sup>2</sup>, and further assess its versatility with other

Table 1: **Implementation details.** The batch size ( $P, K$ ) denotes  $P$  subjects and  $K$  sequences per subject. The parameters  $dr$ ,  $lr$ , and  $wd$  refer to the decay rate, learning rate, and weight decay, respectively.

Dataset	Batch Size	Optimizer	Steps
SUSTech1K	(8, 4)	Adam ( $dr=0.1$ )	50K
CCPG	(8, 8)	$lr=1e-4$	60K
GREW	(32, 2)	$wd=5e-4$	180K
Gait3D	(32, 2)		60K

Table 2: Performance comparisons on SUSTech1K. The **best** and second-best results are highlighted in bold and underlined, respectively.

Modality	Method	Venue	Probe Sequence (R-1)								Overall	
			NM	BG	CL	CR	UB	UN	OC	NT	R-1	R-5
Silhouette	GaitSet	AAAI19	69.1	68.2	37.4	65.0	63.1	61.0	67.2	23.0	65.0	84.8
	GaitPart	CVPR19	62.2	62.8	33.1	59.5	57.2	54.8	57.2	21.7	59.2	80.8
	GaitGL	ICCV21	67.1	66.2	35.9	63.3	61.6	58.1	66.6	17.9	63.1	82.8
	GaitBase	CVPR23	81.5	77.5	49.6	75.8	75.5	76.7	81.4	25.9	76.1	89.4
	DeepGaitV2	TPAMI25	83.5	79.5	46.3	76.8	79.1	78.5	81.1	27.3	77.4	90.2
Silhouette + Skeleton	BiFusion	MTAP24	69.8	62.3	45.4	60.9	54.3	63.5	77.8	33.7	62.1	83.4
	SkeletonGait++	AAAI24	85.1	82.9	46.6	81.9	80.8	82.5	86.2	47.5	81.3	95.5
Silhouette	<b>Ours</b>	-	<b>87.9</b>	<b>84.5</b>	<b>55.4</b>	<b>82.8</b>	<b>87.2</b>	<b>85.1</b>	<b>88.7</b>	<u>38.6</u>	<b>83.8</b>	<b>95.8</b>

baselines, including GaitSet (Chao et al., 2019), GaitGL (Lin et al., 2021), and GaitBase (Fan et al., 2023). (3) Dataset-specific configurations are provided in Table 1. To ensure fairness, the batch size is halved due to the reuse of the discriminative extractor. (4) The generative diffusion module comprises convolution layers, LeakyReLU activations, batch normalization, upsampling (via linear interpolation), and spatial max pooling. Further architectural details are present in Appendix A. (5) The number of continuous frames  $m$  in Equation 6 is fixed to 5. (6) All experiments are conducted on Nvidia GeForce RTX 3090 GPUs.

### 4.3 QUANTITATIVE RESULTS

**Evaluation on SUSTech1K and CCPG.** We compare CoD<sup>2</sup> with several recent methods (Chao et al., 2019; Fan et al., 2020; Lin et al., 2021; Fan et al., 2023; 2025; Peng et al., 2024b; Fan et al., 2024) on the SUSTech1K and CCPG datasets. These results underscore the superiority of CoD<sup>2</sup>. Key observations from Table 2 are as follows:

(1) Silhouette-based methods perform poorly under low-light conditions, achieving a maximum accuracy of only 27.3%, primarily due to degraded image quality caused by insufficient lighting. Despite this, CoD<sup>2</sup> consistently outperforms these methods across all conditions, with a notable improvement of +11.3% under the night condition compared to DeepGaitV2, which achieves the second-highest accuracy (silhouette-based methods) at 27.3%. This highlights CoD<sup>2</sup>’s enhanced ability to extract discriminative features, especially in challenging low-quality silhouette scenarios, such as those encountered at night. (2) CoD<sup>2</sup> achieves state-of-the-art results in most conditions (seven out of eight), outperforming SkeletonGait++ (a multimodal-based method), demonstrating that our method effectively leverages silhouette data alone without relying on additional modalities.

In Table 3, CoD<sup>2</sup> achieves SOTA results across all scenarios, with an average Rank-1 accuracy of 84.8%. This demonstrates that CoD<sup>2</sup> effectively combines the strengths of discriminative and generative models, significantly improving the discriminative model under various clothing conditions.

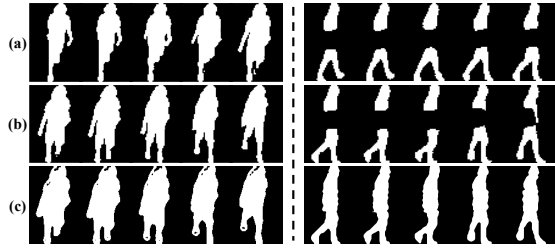
**Evaluation on GREW and Gait3D.** The results on the challenging GREW and Gait3D datasets, summarized in Table 4, demonstrate that CoD<sup>2</sup> outperforms all previous methods. Specifically, on GREW, CoD<sup>2</sup> surpasses VPNet and CLTD by +1.2% and +3.2%, respectively, achieving a Rank-1 accuracy of 81.2%. On Gait3D, CoD<sup>2</sup> improves upon VPNet by +2.9% and WaveLoss (Wang & Wu, 2025) by +2.7%, reaching a Rank-1 accuracy of 78.3%. Importantly, CoD<sup>2</sup> significantly outperforms its baseline, DeepGaitV2, with improvements of +3.5% on GREW (81.2% vs. 77.7%) and +3.9% on Gait3D (78.3% vs. 74.4%). These results further validate the effectiveness of CoD<sup>2</sup> in extracting discriminative gait features under real-world conditions.

### 4.4 QUALITATIVE RESULTS

Figure 4 illustrates that the generated sequences closely resemble the original ones, demonstrating the effectiveness of our generative diffusion module in synthesizing realistic gait sequences. This

Table 4: Performance comparisons on GREW and Gait3D.

Method	Venue	GREW		Gait3D	
		Rank-1	Rank-5	Rank-1	mAP
GaitSet	AAAI19	46.3	63.6	36.7	30.0
GaitPart	CVPR19	44.0	60.7	28.2	21.6
GaitGL	ICCV21	47.3	63.6	29.7	22.3
SMPLGait	CVPR22	-	-	46.3	37.2
DANet	CVPR23	-	-	48.0	-
GaitBase	CVPR23	60.1	-	64.6	-
GaitGCI	CVPR23	68.5	80.8	50.3	39.5
HSTL	ICCV23	62.7	76.6	61.3	55.5
DyGait	ICCV23	71.4	83.2	66.3	56.4
QAGait	AAAI24	59.1	74.0	67.0	56.5
VPNet	CVPR24	80.0	89.4	75.4	-
CLTD	ECCV24	78.0	87.8	69.7	-
WaveLoss	AAAI25	-	-	75.6	66.5
DeepGaitV2	TPAMI25	77.7	87.9	74.4	65.8
<b>Ours</b>	-	<b>81.2</b>	<b>90.8</b>	<b>78.3</b>	<b>71.2</b>

Figure 4: **Visualization of the generated sequence.** From top to bottom, sequences represent  $X_0^m$ , the ground truth of  $X_t^n$ , and  $\hat{X}_0^n$  in Figure 2, respectively.

success is attributed to the integration of visual details (*e.g.*, appearance and motion) with high-level identity-aware semantic information. The visualizations also highlight the discriminative extractor’s ability to learn discriminative gait features, even when the generated sequences deviate from the originals. Notably, as shown on the right side of Figure 4, the goal of the generative diffusion model is not merely to replicate the ground truth, but to capture and enhance discriminative gait information, thereby improving recognition robustness.

#### 4.5 ABLATION STUDIES

**Versatility of CoD<sup>2</sup>.** Table 5 demonstrates that our method significantly improves performance across four discriminative extractors on four datasets, highlighting the effectiveness and versatility of collaboratively integrating discriminative and generative diffusion models for gait recognition. Notably, we observe that incorporating CoD<sup>2</sup> with non-temporal modeling methods (*e.g.*, GaitSet and GaitBase) yields greater performance improvements compared to temporal modeling methods (*e.g.*, GaitGL, and DeepGaitV2). This is due to the generative diffusion model’s ability to introduce rich temporal dynamics, which particularly benefits non-temporal modeling methods.

Table 5: Performance improvements (Rank-1 accuracy) of CoD<sup>2</sup> across different baselines on four datasets.

Method	SUSTech1K	CCPG	GREW	Gait3D
GaitSet	65.0	64.8	46.3	36.7
+ CoD <sup>2</sup>	71.3 <sup>+6.3%</sup>	68.9 <sup>+4.1%</sup>	54.1 <sup>+7.8%</sup>	44.3 <sup>+7.6%</sup>
GaitGL	63.1	66.2	47.3	29.7
+ CoD <sup>2</sup>	69.9 <sup>+6.8%</sup>	68.9 <sup>+2.7%</sup>	51.5 <sup>+4.2%</sup>	35.7 <sup>+6.0%</sup>
GaitBase	76.1	75.5	60.1	64.6
+ CoD <sup>2</sup>	84.2 <sup>+8.1%</sup>	79.4 <sup>+3.9%</sup>	71.1 <sup>+11.0%</sup>	72.6 <sup>+8.0%</sup>
DeepGaitV2	77.4	83.3	77.7	74.4
+ CoD <sup>2</sup>	83.8 <sup>+6.4%</sup>	84.8 <sup>+1.5%</sup>	81.2 <sup>+3.5%</sup>	78.3 <sup>+3.9%</sup>

Table 6: The ablation study of Multi-level Conditional Control strategy.

High-level	Low-level	SUSTech1K	CCPG	GREW	Gait3D
✗	✗	77.4	83.3	77.7	74.4
✓	✗	81.9	84.0	80.4	77.4
✗	✓	81.3	83.7	79.9	77.2
✓	✓	<b>83.8</b>	<b>84.8</b>	<b>81.2</b>	<b>78.3</b>

**Effectiveness of Multi-level Conditional Control strategy.** Table 6 investigates the impact of the Multi-level Conditional Control strategy. The results indicate that both conditions independently improve recognition accuracy, confirming that the extractor  $\mathcal{D}$  effectively learns discriminative identity features. Moreover, the combination of both conditions leads to even greater performance, underscoring their complementary properties.

**Effectiveness of High-level Control Module.** Table 7 evaluates the effectiveness of High-level Control Module by comparing it with the baseline (low-level conditional control only) and an

Table 7: The ablation study of High-level Control Module.

Method	SUSTech1K	CCPG	GREW	Gait3D
Baseline	81.3	83.7	79.9	77.2
w/ addition	83.0	84.4	80.7	77.6
w/ Ours	<b>83.8</b>	<b>84.8</b>	<b>81.2</b>	<b>78.3</b>

element-wise addition strategy. The results demonstrate that our control strategy outperforms direct element-wise addition, highlighting the advantages of High-level Control Module in improving the identity consistency and quality of generated sequences.

**Impact of the number of continuous frames  $m$ .** The number of continuous frames,  $m$ , plays a crucial role in balancing the low-level visual and high-level semantic conditions. As listed in Table 8, experiments with different values of  $m$  (*i.e.*,  $m \in \{1, 3, 5, 7, 9\}$ ) reveal the following trends: (1) When low-level visual information is highly limited (*i.e.*,  $m = 1$ ), the generative diffusion model struggles to learn discriminative features, resulting in suboptimal performance compared to using a single condition. (2) When  $m$  is too large, the generative diffusion model does not need to learn sufficiently, limiting its ability to guide the discriminative extractor and degrading performance. Based on a comprehensive evaluation across four datasets, we set  $m$  to 5.

Table 8: The ablation study of the number of continuous frames  $m$  in Equation 6.

$m$	SUSTech1K	CCPG	GREW	Gait3D
1	81.2	83.7	79.6	76.9
3	83.3	84.5	80.5	77.6
5	83.8	<b>84.8</b>	<b>81.2</b>	<b>78.3</b>
7	<b>84.0</b>	<b>84.8</b>	80.9	78.0
9	83.4	84.2	80.6	77.8

Table 9: The ablation study of the learnable vector  $\lambda$  in Equation 9.

$\lambda$	SUSTech1K	CCPG	GREW	Gait3D
1	83.2	84.3	80.3	77.4
learnable scalar	83.5	84.4	80.8	77.8
<b>learnable vector</b>	<b>83.8</b>	<b>84.8</b>	<b>81.2</b>	<b>78.3</b>

**Impact of the learnable vector  $\lambda$ .** Table 9 compares different strategies for  $\lambda$  (*i.e.*, a fixed value, a learnable scalar, and our learnable vector) in Equation 9. The results show that using a learnable weight to control the adjustment intensity generally enhances recognition performance. Furthermore, the learnable vector achieves the best results, as it allows for adaptive adjustments across different channels.

**Training and Testing Resource Consumption.** Table 10 analyzes the resource consumption of our method on Gait3D during both training and testing. While training demands increase by 7.9% to 15.1% compared to baselines (*i.e.*, GaitSet, GaitGL, GaitBase, and DeepGaitV2), the overhead remains acceptable by halving the batch size, despite the reuse of the discriminative extractor and the introduction of the generative diffusion model. Notably, testing resource requirements remain unchanged. The results in Table 5 and Table 10 demonstrate that CoD<sup>2</sup> achieves significant performance gains without compromising testing efficiency.

Table 10: Training and testing resource consumption on Gait3D. Training is calculated across four GPUs, while testing uses a single GPU.

Method	Training (hour)	Testing (second)
GaitSet	0.95	41
+ CoD <sup>2</sup>	1.08 (+13.7%)	41 (+0%)
GaitGL	2.91	43
+ CoD <sup>2</sup>	3.35 (+15.1%)	43 (+0%)
GaitBase	5.83	77
+ CoD <sup>2</sup>	6.29 (+7.9%)	77 (+0%)
DeepGaitV2	9.98	95
+ CoD <sup>2</sup>	10.94 (+9.6%)	95 (+0%)

## 5 CONCLUSION

In this paper, we propose CoD<sup>2</sup>, an novel gait recognition framework that collaboratively combines the data distribution modeling capabilities of diffusion models with the semantic representation learning strengths of discriminative models. We introduce a Multi-level Conditional Control strategy that integrates high-level identity-aware semantic information with low-level visual details

to guide the generation process. Furthermore, ensuring identity consistency of generated sequences enhances the discriminative model’s ability to learn robust gait features. We assess the effectiveness and versatility of CoD<sup>2</sup> on four datasets.

#### ACKNOWLEDGMENTS

This work is supported by National Natural Science Foundation of China (No. 62376102).

#### REFERENCES

Hanqing Chao, Yiwei He, Junping Zhang, and Jianfeng Feng. Gaitset: Regarding gait as a set for cross-view gait recognition. In *Proceedings of the AAAI Conference on Artificial Intelligence*, volume 33, pp. 8126–8133, 2019.

Ling-Hao Chen, Jiawei Zhang, Yewen Li, Yiren Pang, Xiaobo Xia, and Tongliang Liu. Humanmac: Masked motion completion for human motion prediction. In *Proceedings of the IEEE/CVF Conference on Computer Vision and Pattern Recognition*, pp. 9544–9555, 2023.

Huanzhang Dou, Pengyi Zhang, Wei Su, Yunlong Yu, Yining Lin, and Xi Li. Gaitgci: Generative counterfactual intervention for gait recognition. In *Proceedings of the IEEE/CVF Conference on Computer Vision and Pattern Recognition*, pp. 5578–5588, 2023.

Chao Fan, Yunjie Peng, Chunshui Cao, Xu Liu, Saihui Hou, Jiannan Chi, Yongzhen Huang, Qing Li, and Zhiqiang He. Gaitpart: Temporal part-based model for gait recognition. In *Proceedings of the IEEE/CVF Conference on Computer Vision and Pattern Recognition*, pp. 14225–14233, 2020.

Chao Fan, Junhao Liang, Chuanfu Shen, Saihui Hou, Yongzhen Huang, and Shiqi Yu. Opengait: Revisiting gait recognition towards better practicality. In *Proceedings of the IEEE/CVF Conference on Computer Vision and Pattern Recognition*, pp. 9707–9716, 2023.

Chao Fan, Jingzhe Ma, Dongyang Jin, Chuanfu Shen, and Shiqi Yu. Skeletongait: Gait recognition using skeleton maps. In *Proceedings of the AAAI Conference on Artificial Intelligence*, volume 38, pp. 1662–1669, 2024.

Chao Fan, Saihui Hou, Junhao Liang, Chuanfu Shen, Jingzhe Ma, Dongyang Jin, Yongzhen Huang, and Shiqi Yu. Opengait: A comprehensive benchmark study for gait recognition towards better practicality. *IEEE Transactions on Pattern Analysis and Machine Intelligence*, 47(10):8397–8414, 2025.

Runyang Feng, Yixing Gao, Tze Ho Elden Tse, Xueqing Ma, and Hyung Jin Chang. Diffpose: Spatiotemporal diffusion model for video-based human pose estimation. In *Proceedings of the IEEE/CVF International Conference on Computer Vision*, pp. 14861–14872, 2023.

Lin Geng Foo, Jia Gong, Hossein Rahmani, and Jun Liu. Distribution-aligned diffusion for human mesh recovery. In *Proceedings of the IEEE/CVF International Conference on Computer Vision*, pp. 9221–9232, 2023.

Yang Fu, Shibei Meng, Saihui Hou, Xuecai Hu, and Yongzhen Huang. Gpgait: Generalized pose-based gait recognition. In *Proceedings of the IEEE/CVF International Conference on Computer Vision*, pp. 19595–19604, 2023.

Xun Guo, Mingwu Zheng, Liang Hou, Yuan Gao, Yufan Deng, Pengfei Wan, Di Zhang, Yufan Liu, Weiming Hu, Zhengjun Zha, et al. I2v-adapter: A general image-to-video adapter for diffusion models. In *ACM SIGGRAPH 2024 Conference Papers*, pp. 1–12, 2024.

Jonathan Ho, Ajay Jain, and Pieter Abbeel. Denoising diffusion probabilistic models. *Advances in Neural Information Processing Systems*, 33:6840–6851, 2020.

Jonathan Ho, Tim Salimans, Alexey Gritsenko, William Chan, Mohammad Norouzi, and David J Fleet. Video diffusion models. *Advances in Neural Information Processing Systems*, 35:8633–8646, 2022.

Xiaohu Huang, Duowang Zhu, Hao Wang, Xinggang Wang, Bo Yang, Botao He, Wenyu Liu, and Bin Feng. Context-sensitive temporal feature learning for gait recognition. In *Proceedings of the IEEE/CVF International Conference on Computer Vision*, pp. 12909–12918, 2021.

Xiaohu Huang, Xinggang Wang, Zhidianqiu Jin, Bo Yang, Botao He, Bin Feng, and Wenyu Liu. Condition-adaptive graph convolution learning for skeleton-based gait recognition. *IEEE Transactions on Image Processing*, 32:4773–4784, 2023.

Dongyang Jin, Chao Fan, Jingzhe Ma, Jingkai Zhou, Weihua Chen, and Shiqi Yu. On denoising walking videos for gait recognition. In *Proceedings of the IEEE/CVF Conference on Computer Vision and Pattern Recognition*, pp. 12347–12357, 2025.

Ozgur Kara, Bariscan Kurtkaya, Hidir Yesiltepe, James M Rehg, and Pinar Yanardag. Rave: Randomized noise shuffling for fast and consistent video editing with diffusion models. In *Proceedings of the IEEE/CVF Conference on Computer Vision and Pattern Recognition*, pp. 6507–6516, 2024.

Chang Li, Qian Huang, and Yingchi Mao. Dd-gcn: Directed diffusion graph convolutional network for skeleton-based human action recognition. In *2023 IEEE International Conference on Multimedia and Expo (ICME)*, pp. 786–791. IEEE, 2023a.

Na Li and Xinbo Zhao. A strong and robust skeleton-based gait recognition method with gait periodicity priors. *IEEE Transactions on Multimedia*, 25:3046–3058, 2022.

Weijia Li, Saihui Hou, Chunjie Zhang, Chunshui Cao, Xu Liu, Yongzhen Huang, and Yao Zhao. An in-depth exploration of person re-identification and gait recognition in cloth-changing conditions. In *Proceedings of the IEEE/CVF Conference on Computer Vision and Pattern Recognition*, pp. 13824–13833, 2023b.

Rijun Liao, Shiqi Yu, Weizhi An, and Yongzhen Huang. A model-based gait recognition method with body pose and human prior knowledge. *Pattern Recognition*, 98:107069, 2020.

Beibei Lin, Shunli Zhang, and Xin Yu. Gait recognition via effective global-local feature representation and local temporal aggregation. In *Proceedings of the IEEE/CVF International Conference on Computer Vision*, pp. 14648–14656, 2021.

Huan Ling, Seung Wook Kim, Antonio Torralba, Sanja Fidler, and Karsten Kreis. Align your gaussians: Text-to-4d with dynamic 3d gaussians and composed diffusion models. In *Proceedings of the IEEE/CVF Conference on Computer Vision and Pattern Recognition*, pp. 8576–8588, 2024.

Kang Ma, Ying Fu, Dezhi Zheng, Chunshui Cao, Xuecai Hu, and Yongzhen Huang. Dynamic aggregated network for gait recognition. In *Proceedings of the IEEE/CVF Conference on Computer Vision and Pattern Recognition*, pp. 22076–22085, 2023.

Kang Ma, Ying Fu, Chunshui Cao, Saini Hou, Yongzhen Huang, and Dezhi Zheng. Learning visual prompt for gait recognition. In *Proceedings of the IEEE/CVF Conference on Computer Vision and Pattern Recognition*, pp. 593–603, 2024.

Guozhen Peng, Yunhong Wang, Yuwei Zhao, Shaoxiong Zhang, and Annan Li. Glgait: a global-local temporal receptive field network for gait recognition in the wild. In *Proceedings of the 32nd ACM International Conference on Multimedia*, pp. 826–835, 2024a.

Yunjie Peng, Kang Ma, Yang Zhang, and Zhiqiang He. Learning rich features for gait recognition by integrating skeletons and silhouettes. *MTAP*, 83(3):7273–7294, 2024b.

Ekkasit Pinyoanuntapong, Ayman Ali, Pu Wang, Minwoo Lee, and Chen Chen. Gaitmixer: skeleton-based gait representation learning via wide-spectrum multi-axial mixer. In *ICASSP 2023-2023 IEEE International Conference on Acoustics, Speech and Signal Processing (ICASSP)*, pp. 1–5. IEEE, 2023.

Alireza Sepas-Moghaddam and Ali Etemad. Deep gait recognition: A survey. *IEEE transactions on pattern analysis and machine intelligence*, 45(1):264–284, 2022.

Chuanfu Shen, Chao Fan, Wei Wu, Rui Wang, George Q Huang, and Shiqi Yu. Lidargait: Benchmarking 3d gait recognition with point clouds. In *Proceedings of the IEEE/CVF Conference on Computer Vision and Pattern Recognition*, pp. 1054–1063, 2023.

Jiaming Song, Chenlin Meng, and Stefano Ermon. Denoising diffusion implicit models. In *International Conference on Learning Representations*, 2021.

Wenfeng Song, Xinyu Zhang, Shuai Li, Yang Gao, Aimin Hao, Xia Hou, Chenglizhao Chen, Ning Li, and Hong Qin. Hoianimator: Generating text-prompt human-object animations using novel perceptive diffusion models. In *Proceedings of the IEEE/CVF Conference on Computer Vision and Pattern Recognition*, pp. 811–820, 2024.

Noriko Takemura, Yasushi Makihara, Daigo Muramatsu, Tomio Echigo, and Yasushi Yagi. Multi-view large population gait dataset and its performance evaluation for cross-view gait recognition. *IPSJ transactions on Computer Vision and Applications*, 10:1–14, 2018.

Torben Teepe, Ali Khan, Johannes Gilg, Fabian Herzog, Stefan Hörmann, and Gerhard Rigoll. Gaitgraph: Graph convolutional network for skeleton-based gait recognition. In *2021 IEEE international conference on image processing (ICIP)*, pp. 2314–2318. IEEE, 2021.

Torben Teepe, Johannes Gilg, Fabian Herzog, Stefan Hörmann, and Gerhard Rigoll. Towards a deeper understanding of skeleton-based gait recognition. In *Proceedings of the IEEE/CVF Conference on Computer Vision and Pattern Recognition (CVPR) Workshops*, pp. 1569–1577, 2022.

Aysim Toker, Marvin Eisenberger, Daniel Cremers, and Laura Leal-Taixé. Satsynth: Augmenting image-mask pairs through diffusion models for aerial semantic segmentation. In *Proceedings of the IEEE/CVF Conference on Computer Vision and Pattern Recognition*, pp. 27695–27705, 2024.

Ibrahim Venkat and Philippe De Wilde. Robust gait recognition by learning and exploiting sub-gait characteristics. *International Journal of Computer Vision*, 91(1):7–23, 2011.

Mathias Vogel, Keisuke Tateno, Marc Pollefeys, Federico Tombari, Marie-Julie Rakotosaona, and Francis Engelmann. P2p-bridge: Diffusion bridges for 3d point cloud denoising. In *European Conference on Computer Vision*, pp. 184–201. Springer, 2024.

Jilong Wang, Saihui Hou, Yan Huang, Chunshui Cao, Xu Liu, Yongzhen Huang, and Liang Wang. Causal intervention for sparse-view gait recognition. In *Proceedings of the 31st ACM International Conference on Multimedia*, pp. 77–85, 2023a.

Lei Wang, Bo Liu, Fangfang Liang, and Bincheng Wang. Hierarchical spatio-temporal representation learning for gait recognition. In *Proceedings of the IEEE/CVF International Conference on Computer Vision*, pp. 19639–19649, 2023b.

Ming Wang, Xianda Guo, Beibei Lin, Tian Yang, Zheng Zhu, Lincheng Li, Shunli Zhang, and Xin Yu. Dygait: Exploiting dynamic representations for high-performance gait recognition. In *Proceedings of the IEEE/CVF International Conference on Computer Vision*, pp. 13424–13433, 2023c.

Zengbin Wang, Saihui Hou, Man Zhang, Xu Liu, Chunshui Cao, Yongzhen Huang, Peipei Li, and Shibiao Xu. Qagait: Revisit gait recognition from a quality perspective. In *Proceedings of the AAAI Conference on Artificial Intelligence*, volume 38, pp. 5785–5793, 2024.

Zicheng Wang and Qiuxia Wu. Waveloss: An adaptive dynamic loss for deep gait recognition. In *Proceedings of the AAAI Conference on Artificial Intelligence*, volume 39, pp. 8259–8267, 2025.

Lehong Wu, Lilang Lin, Jiahang Zhang, Yiyang Ma, and Jiaying Liu. Macdiff: Unified skeleton modeling with masked conditional diffusion. In *European Conference on Computer Vision*, pp. 110–128. Springer, 2024a.

Ruiqi Wu, Liangyu Chen, Tong Yang, Chunle Guo, Chongyi Li, and Xiangyu Zhang. Lamp: Learn a motion pattern for few-shot-based video generation. *arXiv preprint arXiv:2310.10769*, 2023.

Rundi Wu, Ruiqi Gao, Ben Poole, Alex Trevithick, Changxi Zheng, Jonathan T Barron, and Aleksander Holynski. Cat4d: Create anything in 4d with multi-view video diffusion models. In *Proceedings of the IEEE/CVF Conference on Computer Vision and Pattern Recognition*, pp. 26057–26068, 2025.

Wei Wu, Qingnan Fan, Shuai Qin, Hong Gu, Ruoyu Zhao, and Antoni B Chan. Freediff: Progressive frequency truncation for image editing with diffusion models. In *European Conference on Computer Vision*, pp. 194–209. Springer, 2024b.

Haijun Xiong, Yunze Deng, Bin Feng, Xinggang Wang, and Wenyu Liu. Gaitgs: Temporal feature learning in granularity and span dimension for gait recognition. In *2024 IEEE International Conference on Image Processing (ICIP)*, pp. 2410–2416. IEEE, 2024a.

Haijun Xiong, Bin Feng, Xinggang Wang, and Wenyu Liu. Causality-inspired discriminative feature learning in triple domains for gait recognition. In *European Conference on Computer Vision*, pp. 251–270. Springer, 2024b.

Haijun Xiong, Bin Feng, Bang Wang, Xinggang Wang, and Wenyu Liu. Mambagait: Gait recognition approach combining explicit representation and implicit state space model. *Image and Vision Computing*, pp. 105597, 2025.

Jinglin Xu, Yijie Guo, and Yuxin Peng. Finepose: Fine-grained prompt-driven 3d human pose estimation via diffusion models. In *Proceedings of the IEEE/CVF Conference on Computer Vision and Pattern Recognition*, pp. 561–570, 2024.

Dingqiang Ye, Chao Fan, Jingzhe Ma, Xiaoming Liu, and Shiqi Yu. Biggait: Learning gait representation you want by large vision models. In *Proceedings of the IEEE/CVF Conference on Computer Vision and Pattern Recognition*, pp. 200–210, 2024.

Heng Yu, Chaoyang Wang, Peiyi Zhuang, Willi Menapace, Aliaksandr Siarohin, Junli Cao, László Jeni, Sergey Tulyakov, and Hsin-Ying Lee. 4real: Towards photorealistic 4d scene generation via video diffusion models. *Advances in Neural Information Processing Systems*, 37:45256–45280, 2024.

Shiqi Yu, Daoliang Tan, and Tieniu Tan. A framework for evaluating the effect of view angle, clothing and carrying condition on gait recognition. In *18th international conference on pattern recognition (ICPR'06)*, volume 4, pp. 441–444. IEEE, 2006.

Cun Zhang, Xing-Peng Chen, Guo-Qiang Han, and Xiang-Jie Liu. Spatial transformer network on skeleton-based gait recognition. *Expert Systems*, 40(6):e13244, 2023a.

Lvmin Zhang, Anyi Rao, and Maneesh Agrawala. Adding conditional control to text-to-image diffusion models. In *Proceedings of the IEEE/CVF International Conference on Computer Vision*, pp. 3836–3847, 2023b.

Jinkai Zheng, Xinchen Liu, Xiaoyan Gu, Yaoqi Sun, Chuang Gan, Jiyong Zhang, Wu Liu, and Chenggang Yan. Gait recognition in the wild with multi-hop temporal switch. In *Proceedings of the 30th ACM International Conference on Multimedia*, pp. 6136–6145, 2022a.

Jinkai Zheng, Xinchen Liu, Wu Liu, Lingxiao He, Chenggang Yan, and Tao Mei. Gait recognition in the wild with dense 3d representations and a benchmark. In *Proceedings of the IEEE/CVF Conference on Computer Vision and Pattern Recognition*, pp. 20228–20237, 2022b.

Jinkai Zheng, Xinchen Liu, Shuai Wang, Lihao Wang, Chenggang Yan, and Wu Liu. Parsing is all you need for accurate gait recognition in the wild. In *Proceedings of the 31st ACM International Conference on Multimedia*, pp. 116–124, 2023.

Jinkai Zheng, Xinchen Liu, Boyue Zhang, Chenggang Yan, Jiyong Zhang, Wu Liu, and Yongdong Zhang. It takes two: Accurate gait recognition in the wild via cross-granularity alignment. In *Proceedings of the 32nd ACM International Conference on Multimedia*, pp. 8786–8794, 2024.

Yixuan Zhu, Ao Li, Yansong Tang, Wenliang Zhao, Jie Zhou, and Jiwen Lu. Dpmesh: Exploiting diffusion prior for occluded human mesh recovery. In *Proceedings of the IEEE/CVF Conference on Computer Vision and Pattern Recognition*, pp. 1101–1110, 2024.

Zheng Zhu, Xianda Guo, Tian Yang, Junjie Huang, Jiankang Deng, Guan Huang, Dalong Du, Jiwen Lu, and Jie Zhou. Gait recognition in the wild: A benchmark. In *Proceedings of the IEEE/CVF International Conference on Computer Vision*, pp. 14789–14799, 2021.

## A ARCHITECTURE OF GENERATIVE DIFFUSION MODULE

In [Table 11](#), we present the architectural details of the generative module  $\mathcal{G}$ . Each block consists of two convolutional layers, accompanied by batch normalization and LeakyReLU activation.

Table 11: Architecture of the generative diffusion module consists of Blocks. Further, HCM represents the High-level Control Module.

Module	Output size	Kernel size
Block	(32, $T$ , 64, 44)	(7, 5, 5) (5, 3, 3)
Pooling	(32, $T$ , 32, 22)	(1, 2, 2)
HCM	(32, $T$ , 32, 22)	-
Block	(64, $T$ , 32, 22)	(5, 3, 3) (3, 3, 3)
Pooling	(64, $T$ , 16, 11)	(1, 2, 2)
HCM	(64, $T$ , 16, 11)	-
Block	(128, $T$ , 16, 11)	(3, 3, 3) (3, 3, 3)
HCM	(128, $T$ , 16, 11)	-
Block	(64, $T$ , 16, 11)	(3, 3, 3) (3, 3, 3)
HCM	(64, $T$ , 16, 11)	-
UpSample	(64, $T$ , 32, 22)	-
Block	(32, $T$ , 32, 22)	(3, 3, 3) (5, 3, 3)
HCM	(32, $T$ , 32, 22)	-
UpSample	(32, $T$ , 64, 44)	-
Block	(1, $T$ , 64, 44)	(5, 3, 3) (7, 5, 5)
Norm	(1, $T$ , 64, 44)	-

Table 12: Performance improvements on CASIA-B and OU-MVLP datasets.

Method	CASIA-B	OU-MVLP
DeepGaitV2 + CoD <sup>2</sup>	89.6% 89.9% ( <b>+0.3%</b> )	91.9% 92.1 ( <b>+0.2%</b> )

Table 13: Performance improvements (Rank-1 accuracy) of CoD<sup>2</sup> across GaitPart on four datasets.

Method	SUSTech1K	CCPG	GREW	Gait3D
GaitPart + CoD <sup>2</sup>	59.2 65.3 <sup>+6.1%</sup>	68.1 70.4 <sup>+2.3%</sup>	44.0 49.2 <sup>+5.2%</sup>	28.2 34.9 <sup>+6.7%</sup>

## B EXPERIMENTS

### B.1 EVALUATION ON CASIA-B AND OU-MVLP

As shown in [Table 12](#), our method achieves 89.9% and 92.1% on CASIA-B and OUMVLP datasets (Yu et al., 2006; Takemura et al., 2018), respectively, with improvements of 0.3% and 0.2% to DeepGaitV2 (Fan et al., 2025), proving its effectiveness.

### B.2 GAITPART ACROSS COD<sup>2</sup>

As shown in [Table 13](#), we integrate our CoD<sup>2</sup> with GaitPart (Fan et al., 2020) to assess the versatility.